Angewandte Chemie

DOI: 10.1002/ange.200903579

Janus Particles

Janus Particles with Controllable Patchiness and Their Chemical Functionalization and Supramolecular Assembly**

*Xing Yi Ling, In Yee Phang, Canet Acikgoz, M. Deniz Yilmaz, Mark A. Hempenius, G. Julius Vancso, and Jurriaan Huskens**

Janus particles constitute a type of soft matter with different physicochemical properties on opposite sides of the particles.[1] As highlighted by de Gennes in his Nobel lecture in 1991,[2] such asymmetric particles offer unique properties that are impossible to attain with homogeneous or symmetric materials. Janus particles have been used as building blocks[3,4] for the assembly of complex nanostructures,[5,6] as two-phase stabilizers,[1,7–10] and for applications in nanomotors,[11] gene delivery,[12] imaging probes,[13] and electronic displays.[14–16]

There are several general routes to synthesize Janus particles,[17] including 1) direct chemical synthetic routes,[18–20] 2) indirect chemical modification of particles at biphasic interfaces,[21–25] and 3) topographically selective modification of particles.[14,21,26–28] Topographically selective modification can be divided into masking/unmasking techniques,[26] direct metal sputtering,[14] microcontact printing,[27] gel trapping,[28] and oil–water emulsion methods.[21] The masking/unmasking technique for selective modification of particles is particularly promising to control the coverage of chemical functionalities (patchiness) on the resulting Janus particles. It involves partial embedding (protection) of a monolayer of particles in a thin layer of a polymer matrix while the exposed surface of the particles undergoes chemical or physical modification. Control over the exposed surface area for surface modification has been demonstrated through thermal control of the volume of embedded silica particles within a polymer matrix[29] and by reactive ion etching to remove the photoresist with a variable etching rate and subsequent local metal deposition.[26]

To date, only basic chemical functionalizations of such particles have been reported to form dipolar charged (positive and negative charges) or amphiphilic (polar and apolar) Janus particles.[14] Assembly of these Janus particles to form anisotropic particle structures is also limited to basic chemical interactions, such as direct formation of anisotropic particle structures through transfer printing of oppositely charged particles.[30–32] Only recently have responsive Janus (nano)particles been reported, the controlled aggregation of which can be fine-tuned by varying the temperature or pH value.[33,34] The chemical modification of particles possesses great potential, but also poses a significant challenge, to form complex Janus particles and anisotropic particle structures by exploiting complementary chemistry. By manipulating the asymmetric chemical functionality on the particles, it is possible to control directly the dimensions, morphology, and physiochemical properties of such building blocks.

Herein, we demonstrate the formation of a variety of chemically functionalized Janus particles that possess controllable anisotropy (patchiness) with the aid of a masking/unmasking technique. In the second section, controllable anisotropic particle structures are prepared by covalent coupling and solution-based supramolecular recognition-directed assembly of chemically functionalized Janus particles. Oxygen plasma etching has been used to create and control the exposed surface area of the silica particles embedded within a PMMA matrix (Scheme 1), such that the chemical patchiness of the Janus particles can be manipulated. Various local chemical functionalization steps have been performed on these particles to create chemically complex Janus particles, including Janus particles with single and binary chemical functionalities. These Janus particles are covalently coupled with secondary particles to form anisotropic particle structures. Moreover, Janus particles with specific supramolecular "host" and "guest" recognition properties are illustrated. By utilizing the specific noncovalent host–guest interactions, controllable solution-based heterogeneous particle assembly is demonstrated to form highly specific dimers that consist of one-to-one pairs of complementary host- and guest-functionalized particles.

The fabrication of Janus particles and anisotropic particle structures with controllable patchiness is described in Scheme 1. A monolayer of silica particles with 5 μm diameter was deposited by spin-coating them onto a surface. A PMMA layer was spin-coated onto the particle layer to fully embed the silica particles within the polymer matrix. O_2 plasma etching was performed on the sample, which resulted in

---

[*] Dr. X. Y. Ling,[+] C. Acikgoz, M. D. Yilmaz, Prof. J. Huskens
Molecular Nanofabrication Group
MESA+Institute for Nanotechnology, University of Twente
7500 AE Enschede (The Netherlands)
Fax: (+31) 53-489-4645
E-mail: j.huskens@utwente.nl
Homepage: http://mnf.tnw.utwente.nl

Dr. I. Y. Phang,[#] C. Acikgoz, Dr. M. A. Hempenius, Prof. G. J. Vancso
Materials Science and Technology of Polymers Group
MESA+Institute for Nanotechnology, University of Twente
7500 AE Enschede (The Netherlands)

[+] Present address: Department of Chemistry
University of California Berkeley
Berkeley CA 94720 (USA)

[#] Present address: Institute of Materials Research and Engineering
3 Research Link, Singapore 117602 (Singapore)

[**] X.Y.L and J.H. thank the Council for Chemical Sciences of the Netherlands Organization for Scientific Research (NWO-CW, Vidi Vernieuwingsimpuls grant 700.52.423 to J.H.) and the University of Twente for financial support.

Supporting information for this article is available on the WWW under http://dx.doi.org/10.1002/anie.200903579.

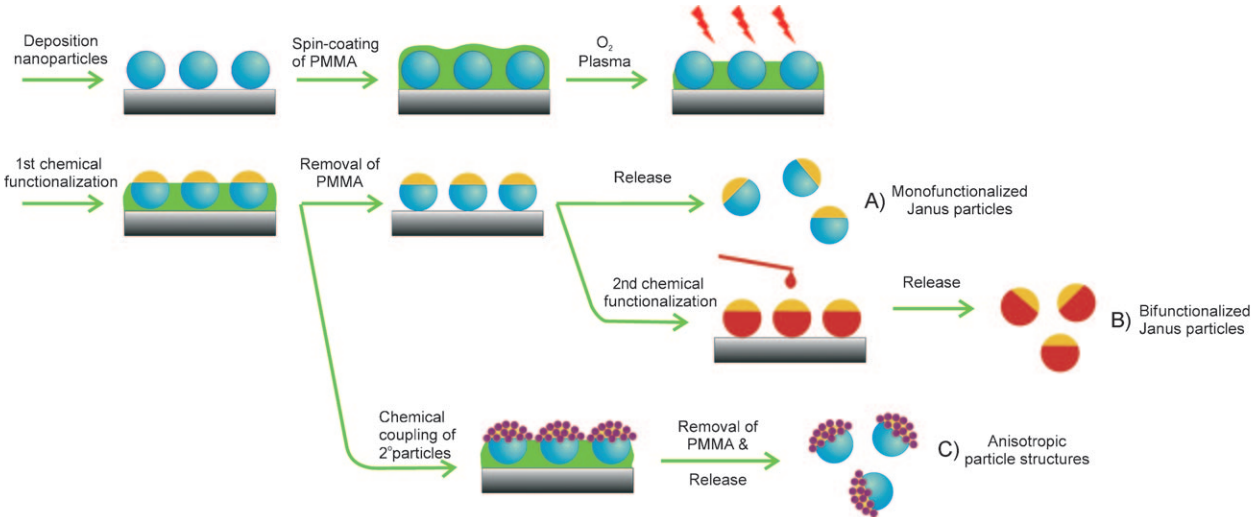

Scheme 1. Preparation of A) mono- and B) bifunctionalized Janus particles and C) anisotropic particle structures by the combination of masking/unmasking and chemical functionalization.

partial removal of the PMMA layer from the sample.[35] This etching created openings in the polymer layer on top of the SiO_2 particles, thus exposing areas of the embedded SiO_2 particles for further chemical modification. By manipulating the duration O_2 plasma etching, we can rationally control the thickness of the removed PMMA layer and the size of the exposed SiO_2 particle surface area. Partial chemical surface functionalization was performed at the exposed surface of the embedded particles to create particles with chemical patchiness. After removal of the remaining PMMA layer by organic solvent, such as acetone, monofunctionalized Janus particles are formed (Scheme 1 A). Upon removal of the remaining PMMA layer, a second chemical functionalization can be performed to form bifunctionalized Janus particles (Scheme 1 B). Furthermore, the asymmetrical chemical functionality of the particles can be further employed for coupling of secondary molecules or nanoparticles, thus forming anisotropic particle structures (Scheme 1 C). The Janus particles or anisotropic particle structures can be released from the surface by sonicating the substrate in water.

Silica particles with 5 μm diameter were used as the main subject of this study for easy visualization of individual particles and differently functionalized areas on these particles by (fluorescence) microscopy. A PMMA layer, equivalent to 280 nm when spin-coated on a flat silicon substrate, was spin-coated onto the monolayer of 5 μm silica particles. Prior to O_2 plasma etching, the particle layer was fully embedded within the polymer matrix. The PMMA-embedded SiO_2 particles retained a similar height profile to that of bare SiO_2 particles, as a result of the very thin layer of PMMA coated on the particles (Figure S1 in the Supporting Information). After exposure to O_2 plasma etching (5–90 s), openings of various sizes were created on the particle surfaces (Figure 1 B–G). This finding indicates that the PMMA layer can be controllably removed to vary the exposed particle area. The top-view diameter of the exposed area of each individual particle across a 50 × 50 μm image area was measured. For 5 s O_2 plasma etching, the diameter of the opening d was 2.2 ± 0.2 μm (Figure 1 I). Upon increase of the etching time, the opening was found to increase correspondingly. At 90 s etching duration, $d = 4.7 \pm 0.2$ μm, thus indicating that almost half of the SiO_2 particle surface area had been cleared of the PMMA mask. By converting d to the fraction of

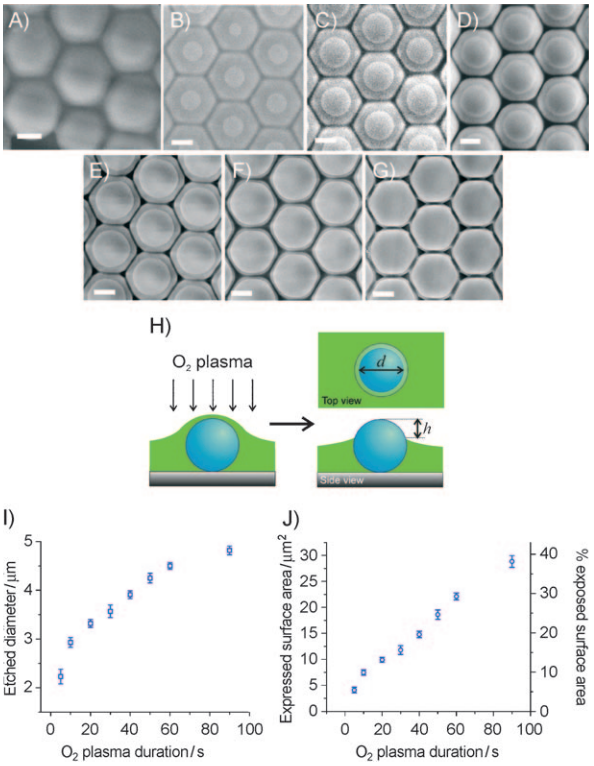

Figure 1. SEM images of the PMMA-embedded SiO_2 particles A) before and B–G) upon O_2 plasma etching for 5 (B), 10 (C), 20 (D), 40 (E), 60 (F), and 90 s (G). Scale bars indicate 2 μm. H) Schematic side and top views of the PMMA-embedded SiO_2 particles upon O_2 plasma etching. Plots of I) etched diameter and J) absolute and relative exposed particle surface area as a function of O_2 plasma etching time.

exposed surface area (Figure 1J), it was found that our technique can systematically control the exposed surface area of the SiO$_2$ particles between about 5 and 40%. The homogeneity of the exposed surface area was excellent over large areas of the substrate, as exemplified by Figure S2 in the Supporting Information. Hence, this procedure allows precise control over the chemical patchiness of the Janus particles upon subsequent chemical functionalization.

The O$_2$-plasma-etched PMMA-embedded SiO$_2$ particles can be generally employed for attaching molecules locally at the exposed surface areas, forming mono- and bifunctionalized Janus particles. By using the 30 s etched PMMA-embedded particles as an example, mono- and bifunctionalized fluorescent particles were prepared. The 30 s etched PMMA-embedded particles were first functionalized with aminopropyltriethoxysilane (APTES) to form NH$_2$-functionalized Janus particles (Figure 2A). Rhodamine molecules were then coupled to the amino layer through a sulfonamide bond using lissamine rhodamine sulfonyl chloride. The rhodamine-functionalized Janus particles were subsequently released into solution by removal of the PMMA layer and sonication in water. The asymmetrical and partial coverage of the rhodamine distribution on the surface of the SiO$_2$ particles is shown in Figure 2B.

The reaction sequence on the substrate-adsorbed particles can be extended to obtain binary fluorescent rhodamine-fluorescein Janus particles. After rhodamine-functionalization and removal of PMMA by organic solvent, a second APTES functionalization was performed on the freshly exposed SiO$_2$ particle surface area (Figure 2A). The second fluorescent dye, fluorescein ester, was subsequently covalently attached. The binary fluorescent Janus particles were released into an aqueous solution for visualization. Fluorescence imaging (Figure 2C) showed the asymmetrical fluorescence properties of the binary fluorescent Janus particles.

Rhodamine is fluorescent upon both green and blue excitation, whereas fluorescein is only fluorescent upon blue excitation. A zoomed-in fluorescence image of the red emission (showing rhodamine only) reveals that the fluorescence intensity of the particle was asymmetrical (Figure 2D). However, upon blue excitation, the entire particle displayed green emission, as both rhodamine and fluorescein are fluorescent under these conditions (Figure 2E). When both fluorescence images were combined (Figure 2F), the partial orange and green fluorescence on the particle can be clearly distinguished, which reveals the distribution of rhodamine and fluorescein.

As a proof of principle, 10 and 90 s etched PMMA-embedded particles, with 10 and 40% exposed surface area, respectively, were used to form anisotropic particle structures (Scheme 1C). Both samples were first functionalized with APTES to form NH$_2$-functionalized Janus particles. A solution containing both carboxylate-functionalized silica nanoparticles ($d \approx 60$ nm) and 1-ethyl-3-(3-dimethylaminopropyl)-1-carbodiimide hydrochloride/*N*-hydroxysuccinimide was cast on the particle layer, with the aim of forming amide bonds between the nano- and microparticles. After ten minutes incubation, the samples were rinsed with water to remove any physisorbed nanoparticles and with dichloro-

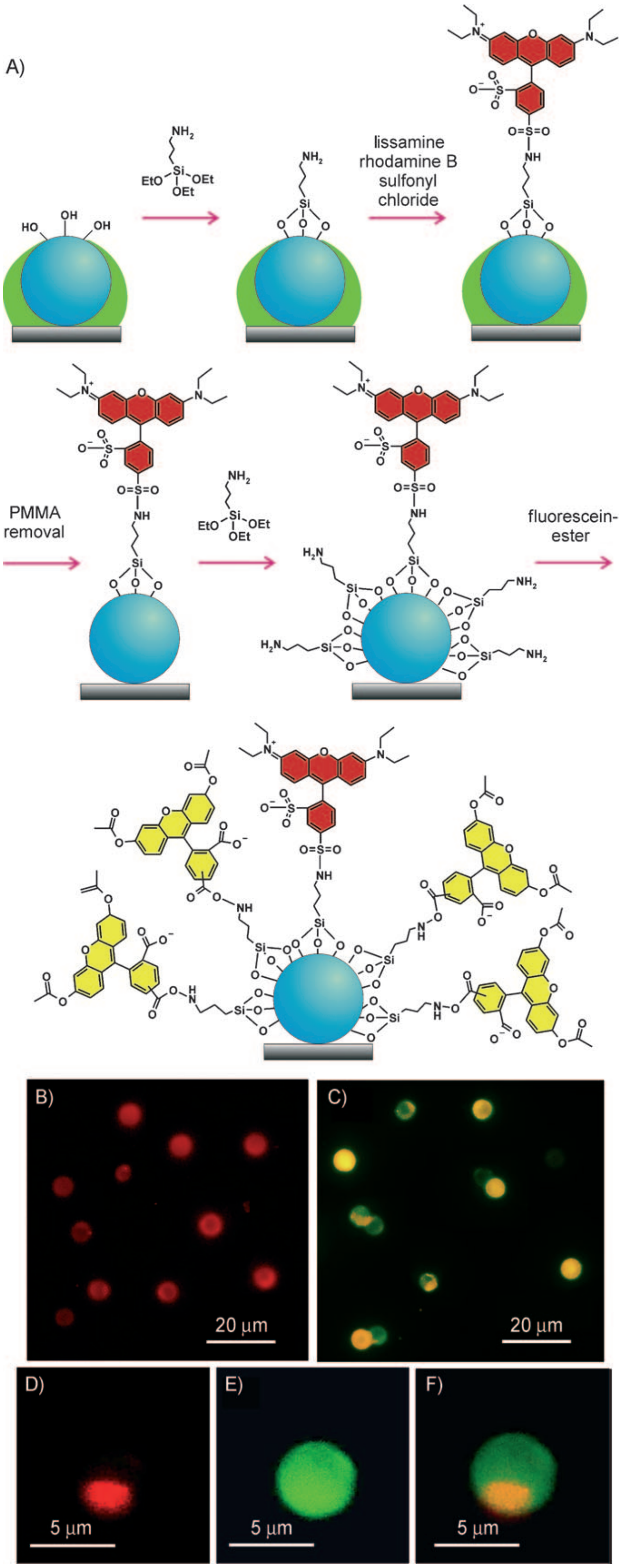

Figure 2. A) The preparation of mono- and bifunctionalized fluorescent Janus particles anisotropically functionalized with rhodamine and fluorescein molecules. Fluorescence microscopy images of B) rhodamine-functionalized Janus particles, C–F) rhodamine- and fluorescein-functionalized binary fluorescent Janus particles showing a combination of red and green emissions (C, F), red emission only (D), and green emission only (E).

methane to remove the PMMA layer. As shown in Figure 3B–E, the sections covered with the nanoparticles corresponded to the microparticle surface areas exposed during etching for both etching times. Apparently, the topographically selective functionalization of the 5 µm silica particle surface and the specific carbodiimide coupling between the NH_2-functionalized Janus particles and ester-functionalized 60 nm silica nanoparticles have resulted in the formation of binary particle structures with tunable patchiness.

The nature of the secondary particles can be varied, thus giving rise to binary anisotropic particle structures with anisotropic material and optical properties. Figure S3 in the Supporting Information shows fluorescence microscopy images of the attachment of carboxylate-functionalized quantum dots (QDs) onto the amino-functionalized anisotropic particle layer (with 5 and 90 s O_2 etching) by carbodiimide coupling. In the case of 5 s etched microparticles, the fluorescence intensity profile directly after chemical modification shows the fluorescence to be concentrated at the center of the silica particles, whereas at the edges of the particles (in top view), the fluorescence intensity is almost negligible (Figure S3 A). In the case of 90 s etched particles, the edges of the particles exhibited a higher fluorescence intensity than the centers of the particles (Figure S3B). This result is attributed to the wider QD coverage on the 90 s etched microparticles, leading to a higher density of QDs in the projected top-view surface area.

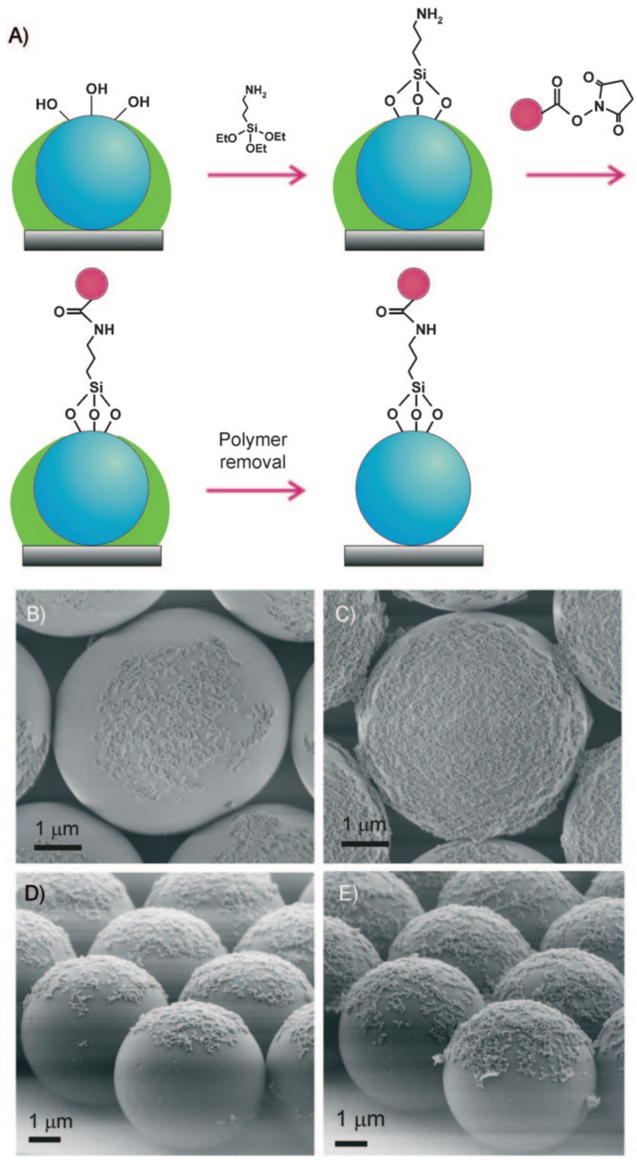

Figure 3. A) The preparation of NH_2-functionalized Janus particles and anisotropic particle structures obtained by carbodiimide coupling with carboxylate-functionalized 60 nm SiO_2 nanoparticles. B–E) SEM images of anisotropic particle structures formed by attaching 60 nm SiO_2 particles to 5 µm amino-functionalized Janus SiO_2 particles by carbodiimide coupling employing O_2 plasma etching for 10 s (B, D) or 90 s (C, E).

The noncovalent supramolecular chemistry involving β-cyclodextrin (CD) and its guest molecules[36–39] has been exploited for the assembly of complementary host- and guest-functionalized Janus particles employing molecular recognition. 10 s etched PMMA-embedded SiO_2 particles were used for making the host- and guest-functionalized Janus particles. Different fluorescent groups were attached on the remaining particle surface areas for fluorescence identification. Figure 4A–D shows the separately prepared host- and guest-functionalized Janus particles. CD-functionalized anisotropic particles (Figure 4A,B) were prepared using a multistep functionalization procedure,[40] and rhodamine was subsequently attached on the remaining areas of the particles, forming binary supramolecular and fluorescent Janus SiO_2 particles. Adamantyl- and fluorescein-functionalized Janus particles (Figure 4C,D) were prepared employing similar synthetic strategies.[37,41] The images in Figure 4B,D show the fluorescence anisotropy of the host- and guest-functionalized Janus particles after release from the substrate and confirm that the different colors allow easy visual identification upon mixing.

By mixing the two complementary particles, the majority of the particles formed dimers (Figure 4E), which consisted of one host-functionalized and one guest-functionalized particle, as indicated by the fluorescent color coding. The yield of perfectly matched supramolecular host-guest anisotropic particle dimers was 50%, as compared to 36% monomeric particles and 14% mismatched particle dimers or trimers. Mismatching may arise from nonspecific hydrophobic dye–dye interactions and can potentially be suppressed by diluting the dye with a hydrophilic molecule in the dye-functionalized areas. Trimers may actually occur through specific interactions when the exposed microparticle surface area functionalized with supramolecular moieties has an angle of greater than 60°, corresponding to an exposed diameter d (Figure 1) of greater than 2.5 µm. The 10 s etching used in this case led to $d = 2.9$ µm and therefore allows some degree of trimer formation. Shorter etching times are needed to suppress trimer formation and to further increase the yield of dimers. Nevertheless, the high yield of matching host–guest particle dimers shows the highly specific recognition-directed assembly in the formation of stable dimers. It is important to note that the results obtained herein differ markedly from the general observation in solution-based supramolecular assem-

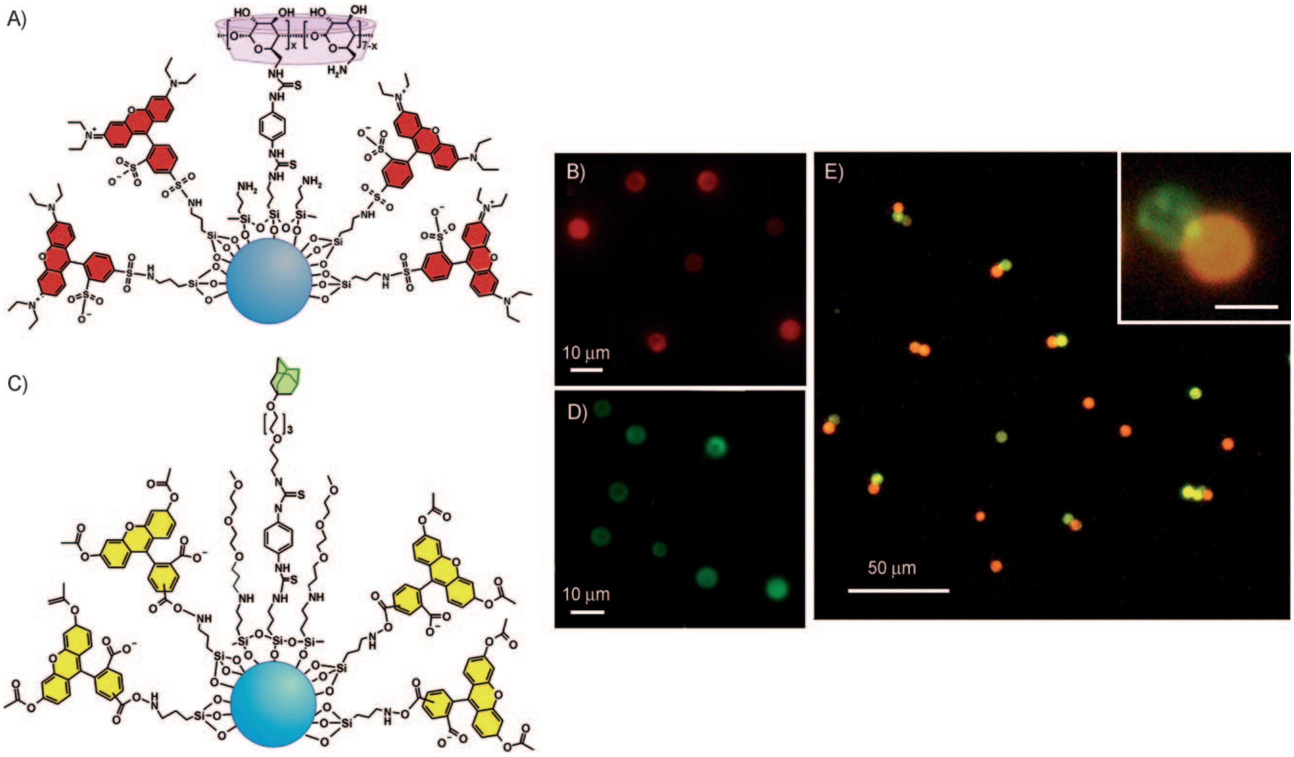

Figure 4. Schematic structures (A, C) and fluorescence microscopy images (B, D) of CD- and rhodamine-functionalized Janus particles (A, B) and of adamantyl- and fluorescein-functionalized Janus particles (C, D), employing 10 s etched PMMA-embedded SiO_2 particles. E) Fluorescence microscopy image after the assembly of the CD- and adamantyl-functionalized anisotropic microparticles by specific host–guest interactions. Scale bar in inset indicates 5 µm.

bly, where uncontrollable aggregation of supramolecular complementary nanoparticles is commonly observed. Our technique allows direct control over the chemical coverage of a particle, where the anisotropic supramolecular properties of the particles result in direct manipulation of the assembly of complementary host- and guest-functionalized particles, even in solution-based aggregation.

In conclusion, preparation of Janus particles with controllable chemical patchiness and anisotropic particle structures with different materials properties, color coding, and recognition properties has been demonstrated. O_2 plasma etching was used to selectively unmask the particles for chemical functionalization, thus allowing the formation of Janus particles with single and binary functionalities. Obviously, the etching method has to be chosen such as not to damage the particle core material. Controlled assembly of Janus particles was demonstrated by manipulating the molecular recognition patchiness on the Janus particles. Our strategy exhibits the potential of such particles with sophisticated asymmetrical chemistries as the basic building blocks for self-assembly of complex structures. They may be further equipped for application as sensors that respond to different environmental stimuli. In particular, the concept of supramolecular Janus particles with controllable molecular recognition properties can be readily applied for the detection of several complementary (bio)molecules simultaneously. Future study will focus on the role of the chemical patchiness of the supramolecular Janus particles in the formation of controlled anisotropic particle structures, such as trimers and larger particle assemblies.

Received: July 1, 2009

Keywords: anisotropic particles · Janus particles · self-assembly · supramolecular chemistry

---

[1] C. Casagrande, P. Fabre, E. Raphael, M. Veyssie, *Europhys. Lett.* **1989**, *9*, 251 – 255.
[2] P. G. de Gennes, *Rev. Mod. Phys.* **1992**, *64*, 645 – 648.
[3] A. Perro, S. Reculusa, S. Ravaine, E. B. Bourgeat-Lami, E. Duguet, *J. Mater. Chem.* **2005**, *15*, 3745 – 3760.
[4] M. Yoshida, J. Lahann, *ACS Nano* **2008**, *2*, 1101 – 1107.
[5] S. C. Glotzer, M. J. Solomon, *Nat. Mater.* **2007**, *6*, 557 – 562.
[6] S. Gangwal, O. J. Cayre, O. D. Velev, *Langmuir* **2008**, *24*, 13312 – 13320.
[7] A. Walther, K. Matussek, A. H. E. Muller, *ACS Nano* **2008**, *2*, 1167 – 1178.
[8] B. P. Binsk, P. D. I. Fletcher, *Langmuir* **2001**, *17*, 4708 – 4710.
[9] S. Jiang, S. Granick, *J. Chem. Phys.* **2007**, *127*, 161102.
[10] S. Jiang, M. J. Schultz, Q. Chen, J. S. Mooret, S. Granick, *Langmuir* **2008**, *24*, 10073 – 10077.
[11] Y. Wang, R. M. Hernandez, D. J. Bartlett, J. M. Bingham, T. R. Kline, A. Sen, T. E. Mallouk, *Langmuir* **2006**, *22*, 10451 – 10456.
[12] A. K. Salem, P. C. Searson, K. W. Leong, *Nat. Mater.* **2003**, *2*, 668 – 671.
[13] M. Yoshida, K.-H. Roh, J. Lahann, *Biomaterials* **2007**, *28*, 2446 – 2456.

[14] H. Takei, N. Shimizu, *Langmuir* **1997**, *13*, 1865–1868.
[15] D. Graham-Rowe, *Nat. Photonics* **2007**, *1*, 248–251.
[16] J. M. Crowley, N. K. Sheridon, L. Romano, *J. Electrost.* **2002**, *55*, 247–259.
[17] A. Walther, A. H. E. Muller, *Soft Matter* **2008**, *4*, 663–668.
[18] V. N. Manoharan, M. T. Elsesser, D. J. Pine, *Science* **2003**, *301*, 483–487.
[19] S. Reculusa, C. Poncet-Legrand, A. Perro, E. Duguet, E. Bourgeat-Lami, C. Mingotaud, S. Ravaine, *Chem. Mater.* **2005**, *17*, 3338–3344.
[20] A. Perro, E. Duguet, O. Lambert, J. C. Taveau, E. Bourgeat-Lami, S. Ravaine, *Angew. Chem.* **2009**, *121*, 367–371; *Angew. Chem. Int. Ed.* **2009**, *48*, 361–365.
[21] K. Fujimoto, K. Nakahama, M. Shidara, H. Kawaguchi, *Langmuir* **1999**, *15*, 4630–4635.
[22] L. Hong, S. Jiang, S. Granick, *Langmuir* **2006**, *22*, 9495–9499.
[23] Y. K. Takahara, S. Ikeda, S. Ishino, K. Tachi, K. Ikeue, T. Sakata, T. Hasegawa, H. Mori, M. Matsumura, B. Ohtani, *J. Am. Chem. Soc.* **2005**, *127*, 6271–6275.
[24] S. Pradhan, L. P. Xu, S. W. Chen, *Adv. Funct. Mater.* **2007**, *17*, 2385–2392.
[25] L. Nie, S. Y. Liu, W. M. Shen, D. Y. Chen, M. Jiang, *Angew. Chem.* **2007**, *119*, 6437–6440; *Angew. Chem. Int. Ed.* **2007**, *46*, 6321–6324.
[26] Z. N. Bao, L. Chen, M. Weldon, E. Chandross, O. Cherniavskaya, Y. Dai, J. B. H. Tok, *Chem. Mater.* **2002**, *14*, 24–26.
[27] O. Cayre, V. N. Paunov, O. D. Velev, *Chem. Commun.* **2003**, 2296–2297.
[28] V. N. Paunov, O. J. Cayre, *Adv. Mater.* **2004**, *16*, 788–791.
[29] C. C. Ho, W. S. Chen, T. Y. Shie, J. N. Lin, C. Kuo, *Langmuir* **2008**, *24*, 5663–5666.
[30] H. Y. Koo, D. K. Yi, S. J. Yoo, D. Y. Kim, *Adv. Mater.* **2004**, *16*, 274–277.
[31] A. T. Skjeltorp, J. Ugelstad, T. Ellingsen, *J. Colloid Interface Sci.* **1986**, *113*, 577–582.
[32] Y. Lu, H. Xiong, X. C. Jiang, Y. N. Xia, M. Prentiss, G. M. Whitesides, *J. Am. Chem. Soc.* **2003**, *125*, 12724–12725.
[33] D. Suzuki, S. Tsuji, H. Kawaguchi, *J. Am. Chem. Soc.* **2007**, *129*, 8088–8089.
[34] T. Isojima, M. Lattuada, J. B. Vander Sande, T. A. Hatton, *ACS Nano* **2008**, *2*, 1799–1806.
[35] C. Acikgoz, X. Y. Ling, I. Y. Phang, M. A. Hempenius, D. N. Reinhoudt, J. Huskens, C. J. Vancso, *Adv. Mater.* **2009**, *21*, 2064–2067.
[36] M. J. W. Ludden, D. N. Reinhoudt, J. Huskens, *Chem. Soc. Rev.* **2006**, *35*, 1122–1134.
[37] X. Y. Ling, D. N. Reinhoudt, J. Huskens, *Langmuir* **2006**, *22*, 8777–8783.
[38] O. Crespo-Biel, B. Dordi, D. N. Reinhoudt, J. Huskens, *J. Am. Chem. Soc.* **2005**, *127*, 7594–7600.
[39] X. Y. Ling, I. Y. Phang, W. Maijenburg, H. Schönherr, D. N. Reinhoudt, G. J. Vancso, J. Huskens, *Angew. Chem.* **2009**, *121*, 1001–1005; *Angew. Chem. Int. Ed.* **2009**, *48*, 983–987.
[40] S. Onclin, A. Mulder, J. Huskens, B. J. Ravoo, D. N. Reinhoudt, *Langmuir* **2004**, *20*, 5460–5466.
[41] L. Basabe-Desmonts, J. Beld, R. S. Zimmerman, J. Hernando, P. Mela, M. F. G. Parajo, N. F. van Hulst, A. van den Berg, D. N. Reinhoudt, M. Crego-Calama, *J. Am. Chem. Soc.* **2004**, *126*, 7293–7299.